TUNING SPEED LIMITATIONS IN WIDE-BAND VARACTOR-TUNED OSCILLATORS*

D. F. Peterson
Electron Physics Laboratory
Department of Electrical and Computer Engineering
The University of Michigan
Ann Arbor, Michigan 48109

ABSTRACT

A technique for studying the transient behavior and tuning speed limitations on wide-band voltage-controlled varactor-tuned oscillators is presented. Analysis of a representative oscillator circuit identifies performance limitations and the tradeoffs between tuning speed, tuning bandwidth, RF power variation and tuning capacitance requirements that can be expected. Experimental results on a 2 to 4 GHz transistor oscillator are presented, indicating 2 ns frequency rise times and associated slew rates of 600 MHz/ns, in good agreement with the theory.

Introduction

Wide-band, fast-tuning, voltage-controlled oscillators (VCO) are a requirement in modern electronic warfare and ECM systems and have great utility in high speed frequency synthesis or control for electronic instrumentation and many other applications. Generally, the performance of these VCOs is measured by such parameters as tuning bandwidth, voltage to frequency linearity, tuning speed or frequency settling time following a tuning voltage step, post-tuning frequency drift, and other related effects. The transient behavior and tuning speed limitations in wide-band varactor tuned VCOs (VTO) are the primary subject of this paper. A simple yet representative oscillator circuit is analyzed, and the results identify the major interactions and tradeoffs between the device, circuit, and tuning varactor without obscuring the problem. The results seem particularly useful for existing lumped-element VTOs which use bipolar transistors, FETs, and Gunn diodes as active devices. Experimental results on the transient behavior of a high speed microwave bipolar transistor oscillator are presented and show good agreement with predictions.

General Properties of Varactor-Tuned Oscillators

A varactor tuned oscillator can generally be represented as indicated in Fig. 1, consisting of a nonlinear active two-terminal or three-terminal device coupled to a nonlinear varactor by a passive network which must additionally provide tuning and load ports. Given the nonlinear properties of the device and varactor, achieving a wide-band, high-speed VTO becomes a coupling circuit design problem, complicated by the nonlinearities involved. Since different active devices and varactors have different nonlinear properties, general statements regarding VTO circuit design should make use of any identifiable common properties these oscillators must have.

Common to most VTO systems are the behavior and location of their natural frequencies in the s-plane under linear or quasi-linear conditions. A wide-band VTO will typically have a natural frequency pattern as shown in Fig. 2 under these conditions. The behavior of these frequencies with changes in varactor capacitance $C_v(V_T)$ and the level of RF in the network can be effectively studied at the varactor port. Under incremental signal conditions the natural frequencies are well defined and are the solutions of (ref. Fig. 1)

$$Z_c(s) + \frac{1}{sC_v(V_T)} = 0 \quad , \qquad (1)$$

which gives a value for $s = s_o(V_T)$ in the right half plane corresponding to the fundamental oscillator natural frequency, in addition to lower frequency solutions $s_v(V_T)$ in the left half plane which characterize coupling to the tuning source. As C_v is charged between its maximum C_{max} and minimum C_{min}, s_o will move essentially parallel to the $j\omega$ axis over as wide a frequency range as the circuit $Z_c(s)$ permits. Likewise, the s_v will vary with C_v depending on the tuning circuit.

Since $R_e\{s_o\} = \sigma_o$ is positive for small signals, the RF amplitude in the circuit will build up as $e^{\sigma_o t}$ until nonlinear saturation effects begin. The saturation can often be adequately described by allowing s_o to be additionally a function of an appropriate RF amplitude A, i.e., $s_o(A,V_T)$, such that a stable oscillator solution occurs when $\sigma_o(A,V_T) = 0$. Equivalently, if A represents the fundamental RF voltage or current amplitude at the varactor port, then $s_o(A,V_T)$ is obtained similarly to Eq. 1 from

$$Z_v(s,V_T,A) + Z_c(s,A) = 0 \quad , \qquad (2)$$

where Z_v and Z_c are now impedance describing functions for the varactor and circuit, respectively. The static tuning behavior and much of the transient behavior can be obtained from the solution $s_o(A,V_T)$ to Eq. 2. Since $R_e\{s_o(A,V_T)\} = \sigma_o(A,V_T)$ is the local growth rate of A(t), then

$$\frac{1}{A}\frac{dA}{dt} = \sigma_o(A,V_T) \qquad (3)$$

is a nonlinear, nonautonomous, "quasi-static" differential equation for A(t) given an initial condition on A and the driving function $V_T(t)$. The solution is termed quasi-static because A(t) typically is slowly varying (a well-defined envelope) over an RF cycle. Having A(t), then the frequency $\omega(t)$ is available as

$$\omega(t) = I_m\{s_o[A(t) \ , \ V_T(t)]\} \quad . \qquad (4)$$

Under steady state conditions when $dA/dt = 0$ and V_T is constant, A and ω become their steady state values A_o and ω_o from Eqs. 3 and 4 indicated in Fig. 2. For the steady-state solution to be stable, the trajectory $s_o(A,V_T)$ vs. A must cross the $j\omega$ axis from left to right as the amplitude increases.

CH1355-7/78/0000-0297$00.75

In general, ω is strongly coupled to variations in $C_v(V_T)$ and weakly coupled to changes in A(t). Hence, $\omega(t)$ is determined primarily by the rate at which the varactor capacitance can be varied by the tuning source. The slower frequency drift coupled to A(t) is zero if the $s_o(A,V_T)$ trajectories vs. A are perpendicular to the $j\omega$ axis.

The tuning speed is set primarily by the location of the s_v in Fig. 2. As $R_e\{s_v\}$ is increased for speed, overall oscillator performance becomes compromised in most practical circuits. For a given active device and oscillator circuit, the tradeoffs between speed and other oscillator parameters can be determined.

Limitations on a Bipolar Transistor Microwave Oscillator

Equivalent Circuit Model

A typical 2 to 4 GHz microwave BJT oscillator utilizes the common collector circuit configuration indicated in Fig. 3. Power is taken at the emitter through a small coupling capacitor, and broadband negative resistance properties occur at the base terminal. A series tuning circuit is appropriate with the varactor series resistance setting the amount of saturation and RF output power. Shown in Fig. 4 are the measured impedance characteristics at the base terminal as a function of frequency and RF current amplitude. From the data, a series representation of the device is appropriate with the reactance effectively modeled by a nonlinear capacitance and a somewhat frequency dependent nonlinear resistance.

Using the device model and associated oscillator tuning circuitry, the simplest circuit for studying the tuning speed limitations is that shown in Fig. 5. Low pass filtering for the tuning circuit is accomplished by the series R-L network, which allows for various damping conditions. This circuit also applies to FET and Gunn diode oscillators in situations when the device is well represented by a series R-C equivalent circuit. The high impedance bias circuit has been neglected and C_B lumped with C_d, so the network of Fig. 5 has four natural frequencies, two lying in the LHP which dominate transient behavior. By varying the circuit elements and moving these poles around in the LHP, various tradeoffs can be established between tuning speed, varactor requirements, device negative Q, and RF power variation across the tuning band.

Performance Limitations and Parameter Tradeoffs

Since the varactor capacitance is nonlinear, the transient response from a high to low frequency is different than that for the reverse transition. Frequency transition times for the system are optimal if the circuit exhibits a critically damped or slightly under damped response around the lowest oscillation frequency f_o. Then an upper bound on the time t_s for the oscillator frequency to get within δf of the final frequency f_2 from an initial frequency f_1 for a step in tuning voltage at t = 0 is obtained from

$$\frac{\delta f}{f_o} = \frac{|f_2 - f_1|}{f_o}(1 + \sigma t_s)e^{-\sigma t_s} , \qquad (5)$$

where σ is the location of the critically damped natural frequency on the real axis in the LHP. Low to high frequency transitions will be underdamped, but will have a t_s less than that given by Eq. 5. A large σ affords small t_s, but with consequences of severe tuning capacitance requirements, large variations in RF power across the tuning band, and oscillator quenching by high frequency energy from the tuning source.

The effects of σ on oscillator performance at oscillation frequency ω are characterized by an operating parameter

$$y(\sigma,\omega) \triangleq \frac{1}{Q_o}\frac{\Delta R_d(\sigma,\omega)}{R_N} , \qquad (6)$$

where R_N is the small signal RF-loop negative resistance $R_d(0) - R_S$, $Q_o = 1/\omega_o C_d R_N$, and $\Delta R_d(\sigma,\omega)$ is the change in steady-state device negative resistance at ω caused by nonzero σ ($\Delta R_d = 0$ when $\sigma = 0$). Since ΔR_d increases with σ and $(\Delta R_d)_{max} = R_N$ or $y_{max} = 1/Q_o$, σ is limited at any frequency in the tuning band. A plot of y versus ω/ω_o is given in Fig. 6 for $\sigma/\omega_o = 0.1$. The parameter is C_d normalized to the varactor capacitance C_{max} necessary for oscillation at ω_o. Any curve above a given device's $1/Q_o$ value represents nonoscillatory circuit conditions, and the difference between y_{max} and any curve is a measure of the RF power level in the circuit. Increased tuning speed (high σ) and reduced RF power variation requires a larger tuning capacitance variation. Typically $C_d/C_{max} \simeq 1$, and about a 7:1 change in varactor capacitance is required for octave-band tuning. In this case σ/ω_o is limited to about 0.1 for typical values of Q_o (7 to 10). Some predicted frequency transients for a step tuning input are shown in Fig. 7. It is evident that frequency slew rates of the order of f_o^2 (Hz/sec) should be achievable for an octave band oscillator.

The nonlinear behavior of $R_d(i)$ is not particularly important as long as the varactor Q and Q_o have typical values, unless σ is allowed to become quite large.

Experimental Results

Using the device curves given in Fig. 4 and an available hyperabrupt varactor, an oscillator as shown in Fig. 3 was constructed to tune from 2.2 to 3.4 GHz for a 0 to 10 V tuning voltage variation. The varactor series resistance of 2.9 Ω determined the RF current amplitude vs. frequency as indicated in Fig. 4.

A tuning circuit was designed to provide a σ/ω_o of 0.07 to have a negligible effect on the fundamental oscillator performance. For this case, appropriate values were R = 100 Ω and L = 50 nH, and the expected frequency risetime to a step in tuning voltage should be about 2.2 ns.

The frequency transients for this circuit were measured at the 50 Ω output using a high speed (0.5 ns risetime) discriminator and a sampling scope, with an avalanche pulse generator (t_r = 0.5 ns) as the tuning input.

Shown in Fig. 8 is the output frequency for the oscillator in response to the tuning pulse. Rise and

fall times for the frequency are about 2 ns as expected (slew rate of 600 MHz/ns) with the underdamped nature of the response around 3.4 GHz and critically damped behavior around 2.2 GHz clearly evident.

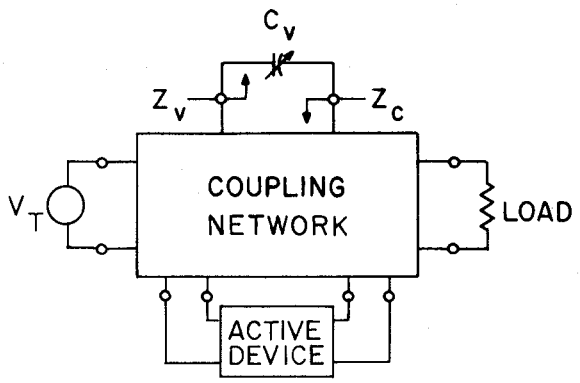

FIG. 1 General Representation of a VTO.

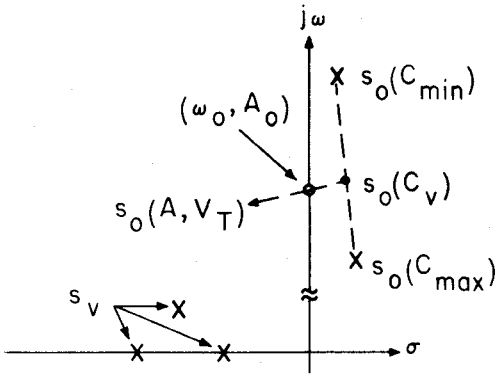

FIG. 2 Typical VTO Natural Frequencies.

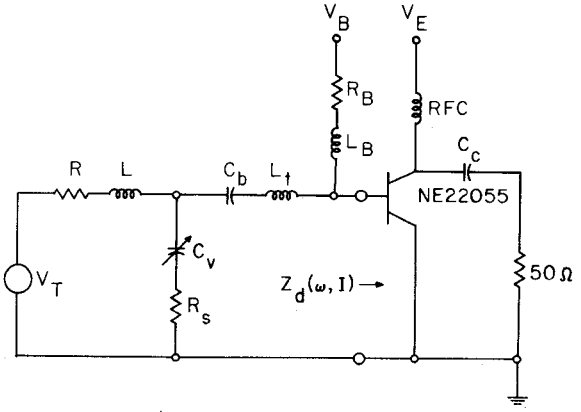

FIG. 3 A 2 to 4 GHz BJT Microwave Oscillator.

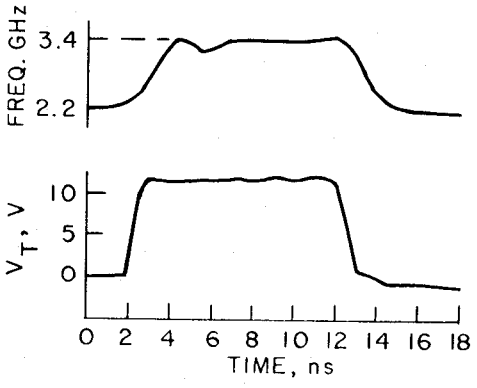

FIG. 8 Measured Oscillator-Frequency Transient Response.

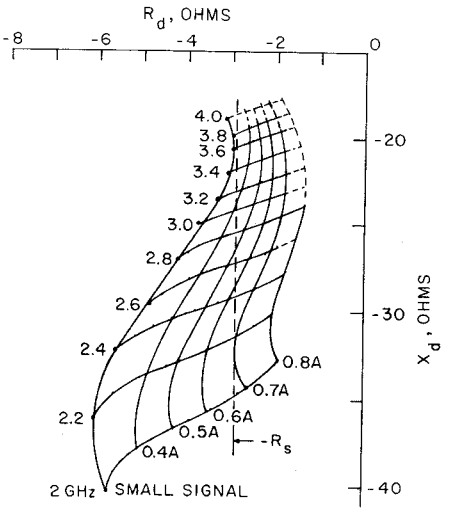

FIG. 4 $Z_d(\omega, I)$ for the Circuit of Fig. 3.

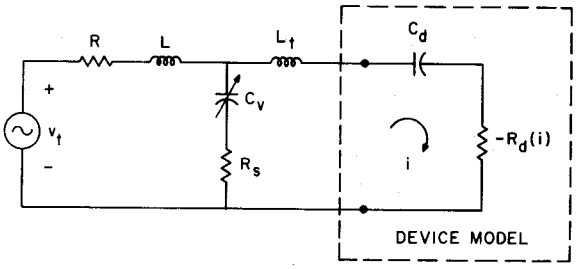

FIG. 5 Circuit Model Used to Study Oscillator Transients.

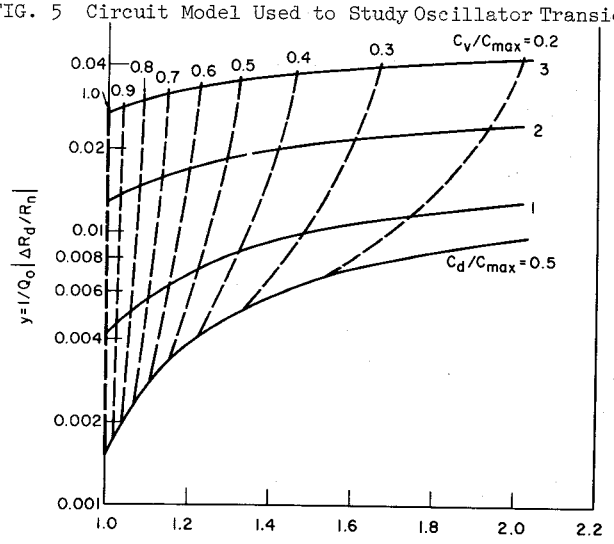

FIG. 6 y Vs. ω/ω_o Various C_d/C_{max} Ratios. (σ/ω_o = 0.1)

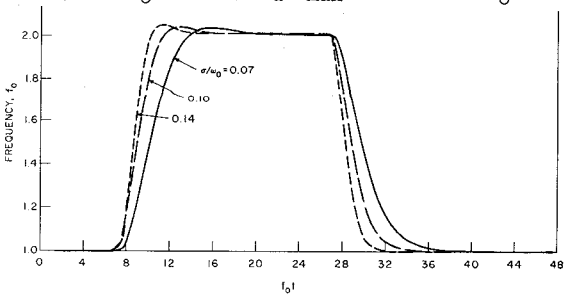

FIG. 7 Theoretical Oscillator-Frequency Transients. (Q_o = 10, C_d/C_{max} = 1)

* This work was supported by Omni Spectra, Inc., Tempe, AZ, under Avionics Laboratory, Wright-Patterson Air Force Base, OH, Subcontract No. A61292-2.